

- (23) Nomura, S.; Kawabata, S.; Kawai, H.; Yamaguchi, Y.; Fukushima, A.; Takahara, H. *J. Polym. Sci.* **1969**, A27, 325.  
 (24) Takayanagi, M.; Imaba, K.; Kajiyama, T. *J. Polym. Sci., Part C: Polym. Symp.* **1966**, 15, 263.  
 (25) Hibi, S.; Maeda, M.; Mizuno, M.; Nomura, S.; Kawai, H. *Sen-i-Gakkaishi* **1973**, 29, 729.  
 (26) Tashiro, K.; Kobayashi, M.; Tadokoro, H. *Macromolecules* **1978**, 11, 914.  
 (27) Matsuo, M. To be submitted.

Registry No. Cellulose, 9004-34-6.

## Excimer Fluorescence as a Molecular Probe of Polymer Blend Miscibility. 9. Effects of Guest Concentration and Annealing in Blends of Poly(2-vinylnaphthalene) with Poly(cyclohexyl methacrylate)

William C. Tao and Curtis W. Frank\*

Department of Chemical Engineering, Stanford University, Stanford, California 94305-5025

Received August 4, 1989

**ABSTRACT:** Excimer fluorescence from poly(2-vinylnaphthalene) (viscosity-average molecular weight of 17 000) was used to study the morphology of blends with poly(cyclohexyl methacrylate) prepared by solvent casting from toluene at 295 K and annealing at 413 K. A lattice model involving three-dimensional electronic excitation transport (EET) was used to interpret the ratio of excimer-to-monomer fluorescence,  $I_D/I_M$ , for P2VN concentration >60 wt %, while an intramolecular one-dimensional EET model was applied to P2VN concentration <25 wt %. Before annealing there is a much higher probability of formation of both intramolecular and intermolecular excimer-forming sites relative to the annealed blend. Furthermore, the blends with P2VN concentration below 70 wt % approach the equilibrium morphology characteristic of 413 K much faster than those with higher concentrations. A concave-downward curvature in  $I_D/I_M$  with increasing P2VN concentration indicates a phase-separated system, while a concave-upward curvature is found for miscible blends. A linear relationship between  $I_D/I_M$  and P2VN concentration can result for miscible blends when there are no intermolecular excimer-forming sites or for immiscible blends, when the volume fraction of the rich phase is much greater than that of the lean phase.

### I. Introduction

Excimer fluorescence is an effective and sensitive morphological tool for the study of miscibility of an aromatic vinyl polymer with a nonfluorescent host polymer.<sup>1-16</sup> A convenient measure of the degree of mixing at the molecular level is the photostationary excimer-to-monomer fluorescence ratio,  $I_D/I_M$ . One problem with establishing excimer fluorescence as a quantitative tool, however, is that there are two photophysical effects that are difficult to separate: the population of traps and the mode by which these traps are sampled. In general, each pendant aromatic chromophore can absorb unpolarized light, and the excitation energy can migrate among the ensemble of chromophores before eventually undergoing non-radiative or radiative decay from a pendant chromophore or lower energy excimer trap.<sup>17</sup> The difficulties in the interpretation of changes in  $I_D/I_M$  with respect to blend thermodynamics stem from the existence of several types of excimer-forming sites (EFS) and the complex pathway of electronic excitation transport (EET) leading to excimer fluorescence. The degree of chain coiling and the extent of guest polymer aggregation will influence both the EFS population and the EET mode by which these traps are sampled. An understanding of the coupled interaction between the number and types of EFS traps and the nature of the excitation transport process is essential to being able to describe the chain structure and the blend morphology.

Our objective is to establish a quantitative understand-

ing of the photophysical properties of the blend of poly(2-vinylnaphthalene) (P2VN) with poly(cyclohexyl methacrylate) (PCMA). To set the stage for this study, we first review the highlights of previous photophysical work on polymer blends and related systems. Initial photophysical work was phenomenological and was based on the simple assumption that the observed  $I_D/I_M$  was proportional to the local concentration of aromatic rings. Phase separation was thus expected to lead to an increase in  $I_D/I_M$ . Experiments were designed based upon the predictions of equilibrium Flory-Huggins thermodynamics.<sup>18</sup>

The first group of experiments by several investigators on relatively high molecular weight polymers emphasized enthalpic contributions to the free energy of mixing. Gashgari and Frank<sup>4-6,9</sup> investigated low-concentration (0.2 wt %) blends of P2VN in a homologous series of poly(alkyl methacrylates) and observed  $I_D/I_M$  to pass through a minimum when the guest and host solubility parameters were equal. Similar results were found for poly(acenaphthylene) and poly(4-vinylbiphenyl) dispersed in the same homologous host matrix series. In addition, Soutar<sup>19</sup> observed a minimum in  $I_D/I_M$  as a function of solvent solubility parameter for poly(1-vinylnaphthalene) and poly(1-vinylnaphthalene-co-methyl methacrylate) in toluene/methanol and toluene/cyclohexane mixed solvent systems. A solvent series was also used by Li et al.<sup>20</sup> to examine  $I_D/I_M$  for polystyrene (PS) labeled with pyrene groups at regularly spaced intervals. In each of these cases, the value of the solubility

parameter for the guest polymer corresponding to the observed  $I_D/I_M$  minimum agrees quite well with literature values or estimates based upon molar group additivity calculation.

The second group of experiments emphasized entropic contributions to the free energy of mixing. The important variable is the molecular weight, which Semerak and Frank<sup>8,11,14</sup> examined for P2VN in both polystyrene and poly(methyl methacrylate) (PMMA) host matrices. The photophysical analysis was still phenomenological with emphasis placed on changes in  $I_D/I_M$  as a function of guest and host molecular weight. However, quantitative calculations of the complete binodal curves using Flory-Huggins theory allowed rationalization of the molecular weight dependence of the apparent microphase separation. The sensitivity of the excimer probe to local blend morphology is demonstrated by the fact that increases in  $I_D/I_M$  consistently preceded changes in the visual appearance of the blends as conditions were altered toward immiscibility.

The third group of experiments moved beyond the phenomenological stage and made the first attempt at treating the photophysics on a quantitative basis. The key element of this work was the development of simple models for EET in limiting concentration regimes. Gelles and Frank<sup>12,13</sup> employed the miscible blend PS/poly(vinyl methyl ether) (PVME) to separate the contribution of EFS population and EET efficiency. A one-dimensional random walk model was used to explain the PS molecular weight dependence of  $I_D/I_M$  for 5 wt % PS blends. A three-dimensional lattice model was used to interpret the  $I_D/I_M$  results for blends with guest concentration >60 wt %. With a two-phase model, they were also able to fit the photostationary data for the immiscible blends cast from tetrahydrofuran (THF). The kinetics of microphase separation were found to be in good agreement with the de Gennes-Pincus theory<sup>21</sup> of spinodal decomposition.

Recent studies have been directed toward nonequilibrium aspects of the solvent-casting process. Frank and Zin<sup>22</sup> observed that the initially cloudy, phase-separated PS/PVME blends cast from THF became clear upon annealing at 384 K and attained the same  $I_D/I_M$  values as those of the miscible PS/PVME blends cast from toluene. The role of the THF in setting up the morphology of the PS/PVME blend is uncertain, but it appears that the blend approaches its equilibrium morphology during the annealing process. Recently, Gashgari and Frank<sup>23</sup> examined the influence of casting temperature on blends of P2VN with poly(*n*-butyl methacrylate) (PnBMA) and PMMA with guest concentration below 10 wt %. They established that solvent casting at temperatures greater than  $T_g$  for the blend/solvent system, followed by rapid quenching to a temperature below  $T_g$ , can quench in the morphology characteristic of the casting temperature. Annealing experiments performed above  $T_g$  on blends cast below  $T_g$  allowed monitoring of the approach to equilibrium.

The present paper is an extension of the Gashgari and Frank<sup>9,23</sup> study in which the effect of annealing at a temperature greater than  $T_g$  is investigated for blends of 71 000  $M_v$  P2VN with PCMA of molecular weight 35 000 over the guest concentration range of 0.1–100 wt %. According to classical differential scanning calorimetry measurements, the PCMA appears to be miscible with P2VN over all proportions. Our first objective is to analyze  $I_D/I_M$  as a function of annealing time with two photophysical models. For results from blends with 60 wt % or greater

P2VN concentration, the Gelles-Frank three-dimensional lattice model should apply. For P2VN concentration <25 wt %, we will test the one-dimensional Fitzgibbon-Frank model.<sup>24</sup> We are particularly interested in the change in the probability of formation of intramolecular and intermolecular EFS as the blends are annealed. The second objective is to use transient-state fluorescence to investigate the efficiency of EET and correlate with the results derived from the photostationary-state models. Finally, we will address the kinetics involved in attaining an equilibrium morphology and discuss the general behavior of the observable  $I_D/I_M$  as a fingerprint for blend miscibility.

## II. Experimental Section

**A. Materials.** Toluene (Aldrich, spectrograde, for fluorescence spectroscopy) was vacuum distilled and passed through a silica gel column prior to use. P2VN (71 000 viscosity-average molecular weight,  $M_w/M_n = 1.30$ ), the same bulk thermally polymerized material described previously,<sup>25</sup> was purified by repeated precipitation from toluene into distilled methanol. PCMA ( $M_n = 35$  000) samples were obtained from Aldrich and purified by repeated precipitation from toluene into distilled methanol.

The solid P2VN/PCMA blends were prepared with toluene as the casting solvent. After the samples were air-dried for 24 h, the initial photostationary-state fluorescence spectra were taken, and the samples were placed in a vacuum oven for annealing. The samples were annealed at 413 K for 12, 24, 48, and 96 h, with spectra being taken at room temperature at the end of each annealing period. To minimize the possibility of oxidative decomposition of the sample during annealing, the oven was evacuated and back-filled several times with nitrogen. The final films were approximately 25  $\mu\text{m}$  thick.

**B. Instrumentation.** The photostationary-state experimental apparatus and methods of P2VN blend investigation have been described elsewhere.<sup>26</sup> Transient fluorescence lifetime measurements were performed on a Photochemical Research Associates nanosecond time-correlated single-photon-counting spectrometer, Model PRA 3000. All of the samples were excited at 290 nm with a 10-nm band-pass excitation monochromator filter. Monomer fluorescence from P2VN, typically observed between 310 and 350 nm, was selectively collected with a Toshiba UV340 10-nm band-pass filter. Instrumental response functions of 1.5-ns fwhm were routinely achieved by collecting the scattered stray light of a Ludox scattering solution at 340 nm, the peak of the monomer emission envelope.

**C. Analysis.** The excimer-to-monomer fluorescence ratio was obtained from intensities measured in regions where overlap between excimer and monomer emission could be neglected. Fluctuations in xenon lamp intensity were corrected for by scaling the data to the exciting beam intensity. The fluorescence spectra were corrected for monochromator and detector response with a tungsten-in-quartz lamp. Transient fluorescence profiles were fitted with a multiexponential trial function by the method of iterative reconvolution with the lamp profile using a nonlinear  $\chi^2$  minimization algorithm of Marquardt.<sup>26</sup> The quality of fit was judged by the reduced  $\chi^2$  criterion, visual inspection of the deviations in the weighted residuals, and the profile of the autocorrelation function.

## III. Results

**A. Annealing Measurements.** The  $I_D/I_M$  results for the P2VN/PCMA blends annealed at 413 K are presented as a function of P2VN guest concentration in Figure 1. Results from the four annealing periods are illustrated along with those from the P2VN/PCMA blends air dried for 24 h. The  $I_D/I_M$  results for 96 h of annealing are identical with those obtained for 48 h. For the blends that were air-dried only,  $I_D/I_M$  is essentially a linear function of P2VN weight percent for P2VN concentration below 80 wt %. The P2VN neat film  $I_D/I_M$

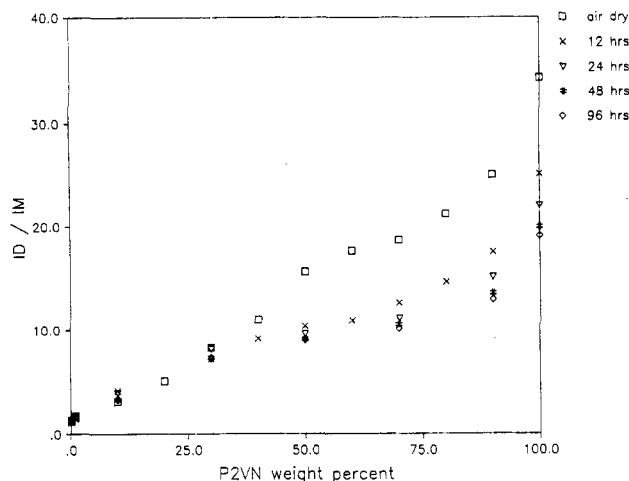


**Figure 1.** Observed  $I_D/I_M$  fluorescence ratio as a function of P2VN guest concentration for blends of P2VN(70 000)/PCMA(35 000) cast with toluene at 295 K. The blends are annealed for a maximum of 96 h at 413 K. The number beside each curve indicates the annealing time. All of the blends remain optically clear after 96 h of annealing. Standard deviations are <10% in this and subsequent plots of  $I_D/I_M$ .

value equals 38, which is about 10% lower than that determined by Semerak.<sup>15</sup> For blends with guest concentration below 30 wt %,  $I_D/I_M$  is independent of annealing time. All of the films are optically clear after air-drying for 24 h, and they remain clear after each annealing period.

The significant point is that  $I_D/I_M$  decreases with annealing time for each P2VN concentration, including the neat film. This suggests that the P2VN configuration in the original cast film is not at equilibrium but frozen in a morphology characteristic of a P2VN/toluene binary system. Semerak and Gashagari<sup>8,9,14</sup> have found that as high as 20 wt % of solvent can remain trapped inside the polymer matrix after air-drying at room temperature for PS and PMMA hosts having glass transition temperatures of 373 and 382 K, respectively. Therefore, it is possible that there could be a large amount of residual toluene left in the blends after 24 h of air-drying.

**B. Transient Fluorescence Lifetimes.** Transient studies of the P2VN/PCMA blends were carried out at room temperature. The decay lifetime of the naphthalene monomer was measured at 340 nm with excitation at 290 nm. In general, the monomer fluorescence decay can be adequately described by a triple-exponential trial function. Tables I–III present the fitted lifetimes and preexponential factors for the different P2VN composition blends that were air-dried and annealed for 12 and 48 h, respectively. These lifetimes cannot be arbitrarily associated with physically distinct excited states. Fredrickson and Frank<sup>27</sup> have shown that a configuration with only a single excimer trap state among many donors can result in a nonexponential decay due to the influence of EET. The form of this nonexponential decay may be approximated as a multiexponential. Our results simply reflect three dominant deactivation pathways for the excited P2VN monomer among the many possible pathways in the complex photophysical scheme.

These dominant deactivation pathways for the monomer have average lifetimes of ca. 5, 25, and 80 ns with intensities of 10%, 25%, and 65%, respectively. The intensity ratios remain relatively constant for the different P2VN composition blends whether or not the blends were annealed. For both the air-dried and annealed blends, the lifetimes decrease with increasing P2VN guest concentration. The lowering of the lifetimes suggests a faster

deactivation of the monomer. This is possibly associated with an increase in the efficiency of EET and the formation of more EFS at high guest concentration.

In the absence of a comprehensive photophysical decay scheme for the P2VN/PCMA blend system, we choose to represent the transient results in the form of a single effective decay lifetime,  $\langle\tau\rangle$ , as a function of blend composition for each of the air-dried and annealed blends. This has been shown to be a good phenomenological approach to relate changes of blend morphology and local polymer interaction to fluorescence results. The effective lifetime is given by

$$\langle\tau\rangle = \frac{\sum A_i \tau_i^2}{\sum A_i \tau_i} \quad (1)$$

where  $A_i$  and  $\tau_i$  are the individual preexponential factor and lifetime. Figure 2 illustrates the calculated  $\langle\tau\rangle$  as a function of P2VN guest concentration for blends that were air-dried and annealed for 12 and 48 h. For blends with P2VN concentration below 50 wt %,  $\langle\tau\rangle$  is essentially constant within experimental error.

## IV. Discussion

**A. Three-Dimensional Electronic Excitation Transport.** The photostationary fluorescence observable may be related to fundamental photophysical quantities by

$$\frac{I_D}{I_M} = \frac{Q_D}{Q_M} \left[ \frac{1-M}{M} \right] \quad (2)$$

where  $Q_D$  is the ratio of the fluorescence decay constant to the total decay constant for the excimer and  $Q_M$  is the analogous ratio for the monomer. The quantity  $M$  is the probability that a photon absorbed by the aromatic vinyl polymer guest will decay along a radiative or nonradiative monomer pathway. Thomas and Frank<sup>16</sup> examined P2VN/PCMA blends and determined that  $Q_D/Q_M$  is equal to  $0.44 \pm 0.08$ . Moreover,  $Q_D/Q_M$  is independent of the host molecular weight, and thus the quantity  $(1-M)/M$  is the only factor that influences  $I_D/I_M$ .

Equation 2 has been applied to polymer blends in two ways. One approach has been to employ an analytical expression for  $M$ , typically containing one or two adjustable parameters, that is thought to be applicable at high or low concentrations of the aryl vinyl polymer. Experimental  $I_D/I_M$  results are then fit with eq 2. This has been done for miscible PS/PVME blends for which the morphology,<sup>12,13</sup> i.e., the random mixing, is relatively uncomplicated. An alternate approach has been taken for the much more complex case of a phase-separated blend. This situation requires that a set of reference data consisting of  $I_D/I_M$  as a function of concentration for a miscible blend of the same components be obtained initially. It is then assumed that the fluorescence behavior of the phase-separated system is a volume-weighted average of contributions to  $M$ , and thus  $I_D/I_M$ , from rich-phase and lean-phase components.

We begin by treating the P2VN/PCMA blend as miscible and analyze the high-concentration results with a three-dimensional spatially periodic lattice model developed by Gelles and Frank,<sup>12,13</sup> referred to as the GF model. This model describes three-dimensional hopping between neighboring sites on a periodic lattice with a distance dependence corresponding to the Förster energy-transfer mechanism for the case of no emission or trapping. The size of the lattice site is taken equal to the size of the P2VN repeat unit; the PCMA segments are then broken up to fit into the same lattice. Under this assumption, the separation distance between adjacent elements

Table I  
Transient Results for Air-Dried P2VN/PCMA Blends

P2VN wt %	A(1)	$\tau(1)$	A(2)	$\tau(2)$	A(3)	$\tau(3)$	$\langle\tau\rangle$	$\chi^2$
10	0.269	6.13	0.157	25.21	0.093	88.03	60.27	1.24
20	0.296	5.27	0.135	25.61	0.099	88.57	63.39	1.32
30	0.297	4.18	0.136	23.34	0.115	84.90	64.05	1.14
40	0.270	4.23	0.144	24.97	0.113	85.24	63.69	1.10
50	0.258	5.08	0.135	26.85	0.107	84.26	61.83	1.12
60	0.257	5.16	0.156	25.59	0.122	81.22	59.97	1.25
70	0.236	4.72	0.153	24.04	0.113	79.37	58.54	1.07
80	0.229	5.17	0.145	24.14	0.113	76.74	56.57	1.12
90	0.231	5.48	0.143	24.92	0.106	76.97	55.72	1.05
100	0.217	4.95	0.146	22.67	0.104	73.62	53.47	1.14

Table II  
Transient Results for P2VN/PCMA Blends Annealed for 12 h

P2VN wt %	A(1)	$\tau(1)$	A(2)	$\tau(2)$	A(3)	$\tau(3)$	$\langle\tau\rangle$	$\chi^2$
10	0.207	5.82	0.104	25.32	0.077	88.65	63.73	1.09
20	0.191	5.67	0.081	26.86	0.074	88.07	65.28	1.08
30	0.179	4.67	0.085	24.04	0.078	84.68	64.45	1.04
40	0.156	5.16	0.085	26.51	0.072	85.30	63.96	0.93
50	0.135	6.23	0.070	28.34	0.066	83.12	62.25	1.18
60	0.125	4.90	0.065	26.06	0.053	80.37	59.15	1.12
70	0.133	5.81	0.075	28.28	0.057	81.08	57.18	0.99
80	0.107	5.13	0.062	24.49	0.046	77.15	55.92	0.90
90	0.107	4.82	0.063	23.31	0.044	74.93	53.87	1.07
100	0.085	3.78	0.039	19.97	0.026	70.90	49.95	1.20

Table III  
Transient Results for P2VN/PCMA Blends Annealed for 48 h

P2VN wt %	A(1)	$\tau(1)$	A(2)	$\tau(2)$	A(3)	$\tau(3)$	$\langle\tau\rangle$	$\chi^2$
10	0.195	5.65	0.102	25.70	0.072	88.42	62.84	1.05
20	0.186	5.49	0.077	27.12	0.071	88.40	65.75	1.01
30	0.165	4.90	0.071	25.79	0.069	85.07	64.70	0.98
40	0.150	4.78	0.067	26.13	0.063	84.77	64.28	1.15
50	0.129	4.52	0.068	25.35	0.057	82.92	62.31	1.21
60	0.121	5.07	0.061	24.47	0.045	80.33	57.68	0.95
70	0.119	4.96	0.053	23.11	0.039	78.21	55.45	1.29
80	0.105	4.55	0.050	22.79	0.032	75.37	52.10	0.97
90	0.099	4.76	0.043	21.96	0.030	74.20	51.66	1.35
100	0.076	3.15	0.034	18.91	0.021	70.11	49.32	1.10

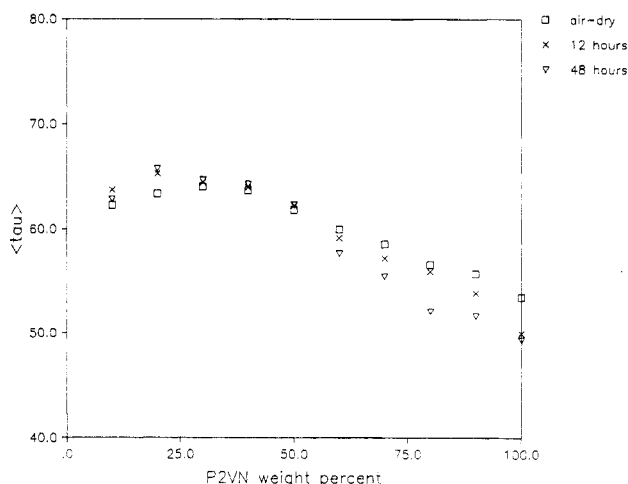


Figure 2. Calculated effective lifetime,  $\langle\tau\rangle$ , for monomer deactivation as a function of P2VN guest bulk concentration. All of the transient fluorescence results can be adequately characterized by a triple-exponential fitting function. The deviation of  $\langle\tau\rangle$  from a constant value for blends with P2VN concentration >50 wt % suggests an enhancement of monomer deactivation possibly due to more EFS formed accompanied by an increase in the dimensionality of EET. The number beside each smooth line drawn through the data indicates the annealing time.

in the lattice will then be constant, although the number of P2VN rings next to any given ring will depend on concentration. It is further assumed that transfer can only take place between rings that are nearest neighbors, that the rate of transfer between two neighbors is

constant with composition, and that the sum of the rates of transfer to each of the nearest neighbors equals the net rate of transfer from a given ring.

The quantity  $M$  takes the form

$$M = \frac{\alpha - q\alpha}{\alpha + q \left[ \frac{1-\alpha}{2-q_D} \right]} \quad (3)$$

where  $q$  is the ring fraction of EFS and is related to the diad trap fraction,  $q_D$ , by  $q = q_D(2 - q_D)$ . The quantity  $\alpha$  is the fraction of times that monomer emission occurs before energy transfer and is given by

$$\alpha = (1 + N\nu W\tau)^{-1} \quad (4)$$

where  $N$  is the number of nearest neighbors of the emitting chromophore in the lattice,  $W$  is the uniform rate of nearest-neighbor EET,  $\tau$  is the measured lifetime of the excitation in the absence of energy transfer, and  $\nu$  is the volume fraction of fluorescent polymer. The diad trap fraction,  $q_D$ , is expressed as the sum of an intramolecular part arising from trans,trans meso rotational diads,  $q_{D,intra}$ , and an intermolecular portion due to segmental association between different chains,  $q_{D,inter}$

$$q_D = q_{D,intra} + q_{D,inter} = q_{D,intra} + (N - 2)\Omega_D\nu \quad (5)$$

The quantity  $\Omega_D$  is the probability that chromophores in two adjacent lattice sites are in an intermolecular EFS.

In order to fit the concentration results for the air-

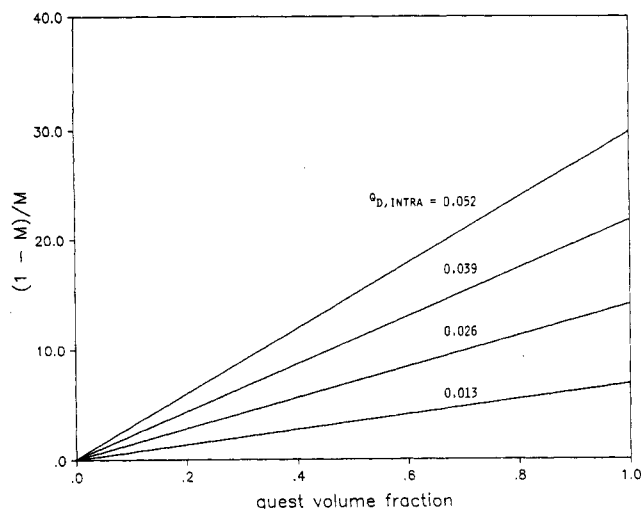


**Figure 3.** Behavior of  $I_D/I_M$  as a function of guest concentration as described by the GF 3-D model for systems with no intermolecular EFS. The number beside each curve indicates the annealing time. The results of the fit are summarized in Table IV.

dried and annealed P2VN/PCMA blends, we have to specify two of the parameters. The quantity  $W\tau$  in Förster dipole-dipole resonant transfer theory is assigned the value corresponding to an average intermolecular chromophore separation of 11.75 Å, which is equal to the Förster radius,  $R_0$ , for a neat P2VN film. We assume that the minimum P2VN concentration at which EET becomes three-dimensional corresponds to this same average intermolecular chromophore separation. At this separation, the probability of transfer between two rings is equal to the probability of monomer emission. If we assume the chromophore separation to be approximately equal to  $[1/(\text{ring concentration})]^{1/3}$ , we obtain the ring concentration corresponding to the onset of three-dimensional EET. From these calculations, we found the P2VN volume fraction to be 0.52. It is interesting to note that similar calculations performed for PS/PVME and P2VN/PnBMA blends indicate that the minimum guest concentration for three-dimensional EET should be 0.60 and 0.14, respectively. Finally,  $N$  is taken to be ca. 10. This leaves  $q_{D,\text{intra}}$  and  $\Omega_D$  as the parameters to be fitted.

It is useful to illustrate graphically the sensitivity of the GF model to variation in the magnitude of  $q_{D,\text{intra}}$  and  $\Omega_D$ . Since both parameters describe the probability of forming more EFS, an increase in either should result in an increase in  $I_D/I_M$ . The effect of these parameters on the efficiency of EET in terms of increased dimensionality, however, is only of second order. Exciton transport is already assumed to be three-dimensional, and the model is expected to be applicable to blends with high guest concentration. It is the frequency of sampling an EFS and the trapping of the exciton that are enhanced.

The behavior of  $I_D/I_M$ , represented in the form of  $(1 - M)/M$  from eq 2, as a function of guest concentration for a varying  $q_{D,\text{intra}}$  is illustrated in Figures 3 and 4. In these calculations, we assumed  $N$  to be 10 and  $W\tau$  to be 51. The latter value has been found by Semerak and Frank<sup>15</sup> to yield a total EFS diad fraction of 0.072 for a neat P2VN film. By comparison, the total EFS diad fraction for pure polystyrene is 0.33. The small EFS fraction for P2VN seems plausible given the low symmetry of the naphthyl pair in forming an EFS. Figure 3 represents the case in which there are no intermolecular EFS, i.e.,  $\Omega_D = 0$ . The linear increase in  $I_D/I_M$  with P2VN volume fraction for any value of  $q_{D,\text{intra}}$  reflects the enhanced sampling of intramolecular EFS on different

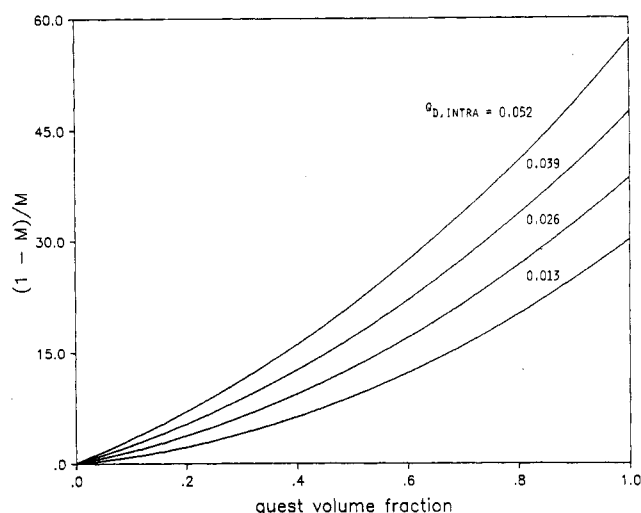


**Figure 4.** Behavior of  $I_D/I_M$  as a function of guest concentration as described by the GF 3-D model for systems with a 0.005 probability for intermolecular EFS formation. The number beside each curve indicates the intramolecular EFS population.

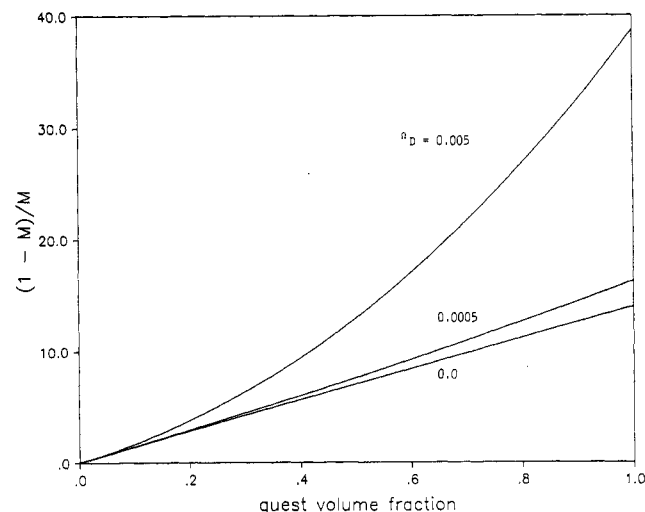


**Figure 5.** Behavior of  $I_D/I_M$  as a function of guest concentration as described by the GF 3-D model for systems with a constant population of intramolecular EFS and different probabilities for intermolecular EFS formation. The number beside each curve indicates the probabilities for forming intermolecular EFS.

chains due to three-dimensional EET. For  $\Omega_D = 0.005$ , shown in Figure 4, there is a substantial increase in  $I_D/I_M$  for the same values of  $\Omega_{D,\text{intra}}$  used in Figure 3. This is better illustrated in Figure 5 in which we keep  $\Omega_{D,\text{intra}}$  constant and vary the magnitude of  $\Omega_D$ . An exciton migrating along a chain contour may encounter a chromophore that can be in an EFS configuration with either an adjacent intramolecular chromophore or an intermolecular chromophore.

The results of fitting the GF model to  $I_D/I_M$  for P2VN/PCMA blends with P2VN concentration >50 wt % are presented in Table IV and illustrated in Figure 6. The model fitted the high-concentration data quite well for the air-dried blends and all of the annealed blends. Both  $\Omega_{D,\text{intra}}$  and  $\Omega_D$  decreased as a function of annealing time. If the lower concentration results are included, we found that the fitting parameters cannot be kept constant over the entire range. Therefore, our choice of P2VN concentration >50 wt % for the applicable range for three-dimensional EET appears to be valid. The magnitude of  $\Omega_D$ , found to be an order of magnitude lower than that for PS in PVME, seems reasonable by comparison due to the strict geometric requirements necessary for inter-

**Table IV**  
Excimer-Forming Site Concentration after Annealing

annealing time, h	$q_{D,intra}$	$\Omega_D$	$q_D^a$
air-dried	0.067	$5.5 \times 10^{-3}$	0.111
12	0.043	$3.9 \times 10^{-3}$	0.074
24	0.046	$3.6 \times 10^{-3}$	0.075
48	0.048	$2.9 \times 10^{-3}$	0.071
96	0.047	$2.9 \times 10^{-3}$	0.070

<sup>a</sup>  $q_D = q_{D,intra} + (N - 2)\Omega_D\nu$ , where  $N = 10$  and  $\nu$  is assigned the value of 1.0.

molecular excimer formation in P2VN.

The results indicate that the air-dried film contains more intramolecular and intermolecular EFS than the annealed film. We infer that it may be in a nonequilibrium state relative to the annealed film. Upon annealing, the blend undergoes diffusive rearrangement, leading to fewer EFS. In Table IV, we present the total EFS concentration for the neat film using the values of  $q_{D,intra}$  and  $\Omega_D$  from the fit. The most important result is that  $q_{D,total}$  starts out higher than the neat film value of 0.072 and approaches a value close to that of the neat film after only a short annealing time. The value of  $q_{D,intra}$  after 12 h of annealing is approximately twice the value calculated from rotational isomeric state theory. This may reflect the influence of guest concentration on the chain configuration of P2VN or additional intramolecular EFS traps beyond the trans,trans meso diad.

The decrease of  $\langle \tau \rangle$  for guest concentration above 50 wt %, as shown in Figure 2, suggests an annealed blend morphology that allows for more efficient monomer deactivation pathways. It is interesting to note that a 50 wt % P2VN blend corresponds to an intermolecular chromophore separation approximately equal to the Förster transfer radius for P2VN. At this chromophore separation, the dominant mode of EET is suspected to be three-dimensional. The decrease in  $\langle \tau \rangle$  might be related to an increase in efficiency of EET due to local rearrangement as the blend is annealed.

We note that  $I_D/I_M$  is independent of annealing time for blends with P2VN concentration below 30 wt %. Our question concerns whether or not the guest coils are sufficiently isolated such that EET among the naphthalene chromophores may be treated as quasi-one-dimensional. If so, the value of  $\Omega_D$  should be much smaller than that found for the high P2VN concentration blends.

A statistical model for strictly one-dimensional exciton migration between nearest neighbors on an isolated polymer chain was originally developed by Fitzgibbon and Frank<sup>24</sup> and will be referred to as the FF model. The FF model treats the equilibrium EFS concentration in the polymer chain as irreversible exciton traps that divide the chain into segments of nontrap sites. In the hypothetical case of an infinitely long polymer chain,  $M$  in eq 2 is computed by averaging the value of  $M$  for each segment length over the distribution of nontrap segment lengths and is given by

$$M = 1 - q_D - \frac{q_D^2}{\tanh(\Gamma)} \sum_{x=1}^{\infty} (1 - q_D)^x \tanh(\Gamma x) \quad (6)$$

where

$$\Gamma = 0.5 \ln \left[ \frac{1 + 2W\tau + (1 + 4W\tau)^{1/2}}{2W\tau} \right] \quad (7)$$

In eq 7,  $q_D$  is the diad fraction of EFS given by eq 5. At the low P2VN concentration for which this model may be appropriate, a first approximation for  $q_D$  is simply the intramolecular site fraction calculated from rotational isomeric state theory.

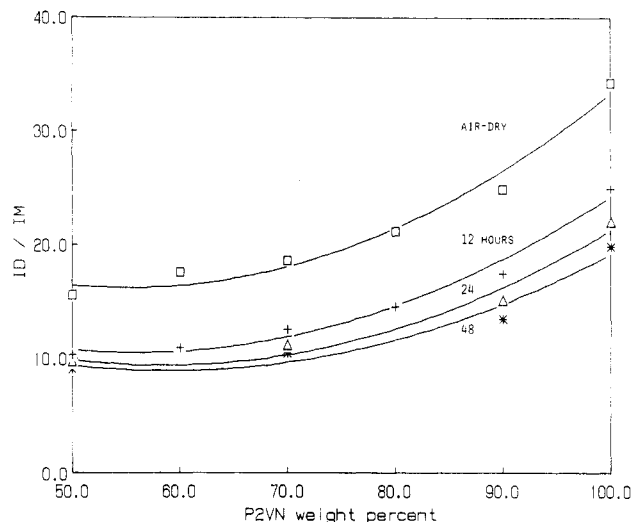


**Figure 6.** Results of fitting the GF 3-D model to the air-dried and annealed blends with P2VN guest concentration >50 wt %. The number beside each curve indicates the annealing time. The results of the fit are summarized in Table IV.

We set  $W\tau$  equal to the Förster value of 51 and  $q_{D,intra}$  to 0.026 as we did for the GF model. The latter value was determined for isolated coils of atactic (45% meso) P2VN. The model is applied over all of the  $I_D/I_M$  results for blends with <30 wt % P2VN, i.e., the linear portion in Figure 1. We realize that this is an ad hoc way of introducing concentration as a parameter in the one-dimensional model, but it is merely intended to test the sensitivity of this model to results from a quasi-one-dimensional system. The value of  $\Omega_D$  from the fit is  $1.72 \times 10^{-5}$ , representing a very low probability of intermolecular EFS formation.

**B. Annealing Kinetics for P2VN/PCMA Blends.** Diffusive rearrangement in a polymer blend depends on the thermal driving force available and the viscosity of the blend. The latter is related to the molecular weight of the blend components, the relative concentration of the polymers, and the amount of residual solvent. During air-drying and annealing, the film composition changes from a ternary system including solvent to that of a binary polymer system. The viscosity of the blend should increase dramatically during this evaporation period, thereby slowing down further changes in local blend morphology.

The thermal driving force is represented approximately by the difference between the annealing temperature,  $T_a$ , and the glass transition temperature of the blend,  $T_g$ . For the P2VN/PCMA system, the glass transition temperature for different blend compositions follows the Fox equation<sup>28</sup>

$$\frac{1}{T_g(\text{blend})} = \frac{w}{T_g(\text{P2VN})} + \frac{1-w}{T_g(\text{PCMA})} \quad (8)$$

where  $w$  is the weight fraction of P2VN. The annealing experiment was performed at a temperature of 413 K, which is 76 K above the  $T_g$  of PCMA and only 8 K above the  $T_g$  of P2VN. From eq 8, it is obvious that the thermal driving force for molecular rearrangement will be greater for the lower P2VN concentration blend.

The general slope of curves between  $I_D/I_M$  and annealing time drawn through the results shown in Figure 1 for a constant P2VN concentration suggests that a fitting equation of the form

$$R[t] - R[96] = \{R[0] - R[96]\} \exp(-kt) \quad (9)$$

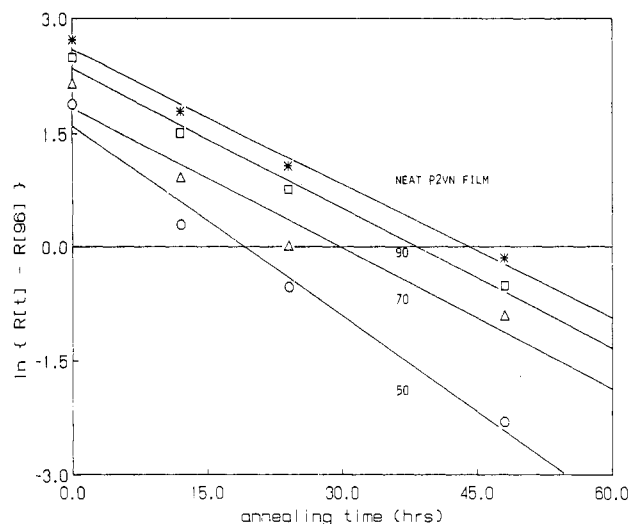


**Figure 7.** Analysis of the effect of annealing time at 413 K for P2VN/PCMA blends cast at 295 K. The smooth lines drawn through the data represent the use of eq 9 to fit the results.

**Table V**  
Rate Constant for Thermal Diffusive Rearrangement

P2VN wt %	$k$ , $\text{h}^{-1}$	$\tau$ , h	$T_a - T_g^a$
100	0.059	16.95	8.0
90	0.061	16.39	16.01
70	0.062	16.13	31.12
50	0.084	11.91	45.16

<sup>a</sup> The  $T_g$  is calculated according to the Fox equation (eq 8).

may be appropriate. Here  $R = I_D/I_M$  and  $R[96]$  is the value of  $I_D/I_M$  after 96 h annealing at 413 K,  $R[t]$  is the ratio after  $t$  hours of annealing,  $R[0]$  is  $I_D/I_M$  for the room temperature cast blend prior to annealing, and  $k$  is the rate constant characterizing the diffusive rearrangement. Representative plots for 50, 70, and 90 wt % P2VN concentration blends and the neat film are presented in Figure 7. In general, this semilogarithmic form fits the data quite well over the entire range of annealing times.

The rate constants derived from the plots of Figure 7 are presented in Table V along with the magnitude of the thermal driving force expressed as  $T_a - T_g$ . It appears that the rate of diffusive rearrangement is limited by the viscosity of the blend until the thermal driving force exceeds 35 K. By comparison in P2VN/PnBMA blends with 10 wt % P2VN, local motion of the polymer with similar time scales occurs at  $T_a - T_g = 20$  K. Although thermally induced phase separation occurs for the P2VN/PnBMA system after annealing, the value of  $T_a - T_g$  still reflects the magnitude of the thermal driving force required to cause diffusive motion between the guest coils. This suggests that the use of the Fox equation to calculate  $T_g$  might be inappropriate for the higher guest concentration blends.

Application of the Fox equation is only appropriate when the blend is homogeneous over the entire range of blend composition. Equation 8 will be inapplicable when the blend is phase separated. We can use the results for the neat P2VN film in Table V as a reference for the following interpretation. For the neat film, thermal annealing at 413 K cannot cause macroscopic phase separation but does provide sufficient driving force for local rearrangement. This type of motion occurs at a time scale equal to ca. 17 h, as shown in Table V. The near-constant rate of diffusive motion for blends with P2VN guest concentration >70 wt % suggests that the thermal driving force for these blends is actually lower than that calculated with eq 8. The local chromophore concentra-

tion resembles that of the neat film, resulting in a higher glass transition temperature for the blend.

**C. Behavior of  $I_D/I_M$  Reflecting the Degree of Blend Miscibility.** In this section we wish to examine the general characteristics of plots between  $I_D/I_M$  and guest concentration for miscible and immiscible blends. The behavior of  $I_D/I_M$  with increasing guest concentration can be classified into three types: linear, concave upward, and concave downward. The PS/PVME blend is a good example in which all three trends have been observed using different casting solvents.<sup>12,13</sup> When cast from chlorobenzene, toluene, and THF,  $I_D/I_M$  exhibits linear, concave-upward and concave-downward curvature with guest concentration, respectively. The blends prepared with toluene have been shown to be miscible for all proportions of PS and PVME, while blends prepared with THF have been shown to be immiscible. It appears that, in general, miscible blends are characterized by a concave-upward trend in  $I_D/I_M$ , and the reverse holds true for immiscible blends. The linear behavior is a limiting case for both types of blends.

For a miscible blend, the EFS concentration and the EET efficiency change slowly as the guest concentration is increased. From Figures 3–5, we observe the effects of changing the EET efficiency in sampling EFS on the curvature of  $I_D/I_M$  with guest concentration. We realize that the GF three-dimensional EET model should only be applied to blends with high guest concentration. Therefore, the extension of the GF model to low guest concentration assumes that the local EFS population is high enough to allow three-dimensional EET to occur. This may be valid for a system of isolated, tightly contracted guest coils dispersed in a poor host matrix. The GF model does not take into account any intramolecular morphological transformation as the guest concentration is increased. We merely intend to assess the qualitative behavior of  $I_D/I_M$  as a function of guest concentration for a miscible blend as the population and types of EFS are altered.

Figure 3 illustrates linear behavior in  $I_D/I_M$  for a system in which there is no intermolecular EFS formation. As the guest concentration increases, the EET process switches from mainly three-dimensional sampling of intramolecular EFS at low concentration to include sampling of intramolecular EFS on nearby chains at high concentration, i.e., cross-chain hopping.  $I_D/I_M$  continues to increase due to this enhanced sampling of intramolecular EFS by the exciton. The slope of the linear  $I_D/I_M$  trace depends on the population of the intramolecular EFS per chain.

It is unrealistic for blends with vinyl aromatic polymer to have no intermolecular EFS at high guest concentration. It is conceivable, however, that specific interactions between the guest polymer and the host or residual solvent in the film could yield a protective clustering around the chromophores, thereby lowering the probability of intermolecular EFS formation. Figure 4 illustrates the effect of introducing a small population of intermolecular EFS on the behavior of  $I_D/I_M$ . The  $I_D/I_M$  trace adopts a concave-upward curvature, especially for higher guest concentration. In addition to the enhanced sampling by three-dimensional EET, there are now more EFS to trap the excitation. The effect of increasing the probability of intermolecular EFS formation for a system with a fixed intramolecular EFS population is shown in Figure 5. In this figure, the transition from linear to concave-upward behavior is more dramatic with a higher probability of forming intermolecular EFS. It is important



to remember that each plot in Figures 3–5 represents systems in which the type and population of each type of EFS are held constant throughout the entire composition range. Our results for the P2VN/PCMA blend system in Figure 1 clearly show a combination of both linear and concave-upward  $I_D/I_M$  behavior due to changing EFS type and population with increasing P2VN concentration.

Polymer blends typically show a decrease in miscibility with increasing temperature. Whether a blend phase separates as part of the diffusive relaxation upon annealing depends on the annealing temperature relative to both the lower critical solution temperature and the glass transition temperature, respectively. For blends of P2VN and PCMA with molecular weights of 71 000 and 35 000, respectively, the annealing temperature of 413 K is probably below the lower critical solution temperature such that the blends remain miscible after annealing. Further annealing at 413 K allows the blend to relax into its equilibrium morphology while maintaining miscibility. The behavior of  $I_D/I_M$ , as shown in Figure 1, remains concave upward after annealing.

Gashgari and Frank<sup>23</sup> examined 71 000  $M_v$  P2VN blended with PnBMA and PMMA. For the P2VN/PnBMA blend  $I_D/I_M$  increased with annealing at 407 K and leveled off after 25 h, while for P2VN/PMMA,  $I_D/I_M$  did not level off even after 160 h of annealing at 407 K. In both cases,  $I_D/I_M$  exhibited a concave-downward curvature as a function of P2VN bulk concentration. An explanation for the behavior of  $I_D/I_M$  as a function of annealing time in these different host matrices is due to thermally induced phase separation in the P2VN/PnBMA and P2VN/PMMA blends. These blends started out as optically cloudy films and remained cloudy after annealing. The increase in  $I_D/I_M$  can be due to an increase in the intermolecular EFS as a result of phase separation or an increase in the nonadjacent intramolecular EFS due to tightening of the polymer coils. The latter is more likely to happen with the P2VN/PMMA blend since it is a thermodynamically less compatible blend compared to P2VN/PnBMA.

In addition to the above two cases, the behavior of  $I_D/I_M$  with guest concentration for PS cast with THF in PVME has been observed to change from an initially concave-downward curvature to a concave-upward profile upon annealing. In this system, the appearance of phase separation is caused by possible kinetic limitations to the attainment of thermodynamic equilibrium, which in turn is due to the influence of residual casting solvent on the morphology of the blend. Zin and Frank<sup>22</sup> annealed PS/PVME blends cast with THF, which was earlier found to be phase separated, and observed a decrease in  $I_D/I_M$  back to values found for miscible PS/PVME blends cast from toluene.

The aggregation of chromophores during phase separation leads to a rapid increase in the population of both intermolecular and nonadjacent intramolecular EFS and favors three-dimensional EET among the chromophores. Overall,  $I_D/I_M$  increases rapidly for small changes in guest concentration and is reflected by a concave-downward behavior. As the P2VN bulk concentration increases, the P2VN-rich domains grow larger but with little change in the EFS population within the phase. Therefore,  $I_D/I_M$  levels out to the neat film value at high guest concentrations.

Gelles and Frank<sup>12,13</sup> have used excimer fluorescence as a molecular probe to determine the morphology and phase concentrations of phase-separated systems such as

PS/PVME blends cast from THF. In deriving a two-phase model of  $I_D/I_M$  for phase-separated blends, they assumed that the volume fractions of the guest in the rich and lean phases,  $\phi_R$  and  $\phi_L$ , are independent of the bulk concentration  $\phi_B$ . They further assumed that there will be no energy migration between phases. This is a good assumption because the guest chains in the lean phase should be sufficiently isolated so that the probability of three-dimensional EET is small, while the excitation in the rich phase should be rapidly trapped due to the high concentration within a concentrated phase that is large enough to scatter light. The problem then is reduced to first determining what fraction of photons is absorbed by each phase and then characterizing the deactivation pathway of an absorbed photon by a phase of known composition.

The resulting expression for  $I_D/I_M$  for a phase-separated blend is given by

$$\frac{I_D}{I_M} = \frac{Q_D}{Q_M} \frac{X_R(1 - M_R) + (1 - X_R)(1 - M_L)}{X_R M_R + (1 - X_R) M_L} \quad (10)$$

where  $X_R$  is the probability that a photon is absorbed by a ring in the rich phase and is given by

$$X_R = \frac{\phi_R(\phi_B - \phi_L)}{\phi_R(\phi_B - \phi_L) + \phi_L(\phi_R - \phi_B)} \quad (11)$$

The quantities  $M_R$  and  $M_L$  are the probabilities of eventual excitation deactivation through a monomer pathway for an absorbed photon originating in the guest-rich and guest-lean phases, respectively. To use eq 10, we must obtain estimates for  $\phi_R$  and  $\phi_L$  at the casting temperature from a phase diagram for the blend, and  $M_R$  and  $M_L$  are determined from the fluorescence data for miscible blends of the same components using eq 2.

Since we require photophysical information from a miscible system to estimate  $M_R$  and  $M_L$ , we need to investigate the influence of  $M$  derived from a miscible blend on the behavior of  $I_D/I_M$  for phase-separated blends. The significant qualitative feature is that  $M$  usually decreases rapidly with increasing guest concentration. This is a consequence of the increase in the number of EFS traps and the expected increase in efficiency of EET due to increased dimensionality of the random walk. The combination of these two effects leads to considerable nonlinearity.

For miscible blends exhibiting a linear, quadratic, or cubic dependence of  $M$  on  $\phi_B$  (i.e., the profile of  $M$  derived from the behavior of  $I_D/I_M$  on  $\phi_B$  using eq 2), it can be shown that eq 10 assumes the form

$$\frac{I_D}{I_M} = \frac{A + B\phi_B}{C + \phi_B} \quad (12)$$

where the constants  $A$ ,  $B$ , and  $C$  represent different algebraic relations between the quantities  $\phi_R$ ,  $\phi_L$ , and  $Q_D/Q_M$ . We will illustrate the derivation of eq 12 for a linear dependence of  $M$  on  $\phi_B$ . It is a straightforward exercise for other functional forms of  $M$  on  $\phi_B$ .

For a miscible system exhibiting a linear dependence of  $I_D/I_M$  on  $\phi_B$

$$I_D/I_M = \alpha' + \beta'\phi_B \quad (13)$$

the parameters  $M_R$  and  $M_L$  assume the following form according to eq 2;

$$M_R = (\alpha + \beta\phi_R)^{-1} \quad (14)$$

$$M_L = (\alpha + \beta\phi_L)^{-1} \quad (15)$$



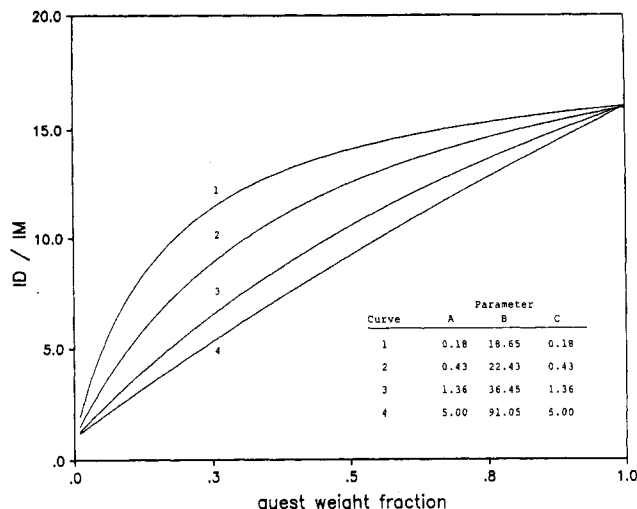


**Figure 8.** Behavior of  $I_D/I_M$  as a function of bulk guest concentration for a phase-separated blend. The concave-downward curves follow the GF two-phase model as described in eq 10–12.

where the constants  $\alpha = (\alpha' + Q_D/Q_M)/(Q_D/Q_M)$  and  $\beta = \beta'/(Q_D/Q_M)$ . Substituting eq 11, 14, and 15 into eq 10 and collecting the terms into the form of eq 12, we find the following forms for the constants A, B, and C:

$$A = \frac{\phi_R \phi_L \{\alpha^2 - \beta \phi_R - \alpha \beta \phi_L - \beta^2 \phi_R \phi_L\}}{(\phi_R - \phi_L)(1 + \alpha)} \quad (16)$$

$$B = \frac{(\phi_R - \phi_L)\alpha(1 + \alpha) + \phi_R^2\{\beta(1 + \alpha) + \beta^2 \phi_L\}}{(\phi_R - \phi_L)(1 + \alpha)} \quad (17)$$

$$C = \frac{\beta \phi_R \phi_L}{1 + \alpha} \quad (18)$$

Using the phase-separated PS/PVME blend cast from THF as an example, we find the quantities  $\phi_R$ ,  $\phi_L$ ,  $\alpha$ , and  $\beta$  have values of 0.98, 0.008, 1.0, and 10, respectively. The behavior of eq 12 as a function of guest concentration for typical values of A, B, and C is shown in Figure 8. The concave-downward trend seems to be intrinsic for phase-separated blends.

## V. Summary

First, we have shown for low molecular weight P2VN/PCMA blends that solvent casting with toluene at room temperature and subsequent evaporation by air-drying lead to a nonequilibrium blend morphology. The latter is characterized by a high population of both intermolecular and intramolecular EFS, which upon annealing at 413 K, approach the equilibrium statistical population. The photostationary-state fluorescence results for

blends with P2VN concentration above 50 wt % are well characterized by a three-dimensional EET model. The effective lifetime for monomer deactivation supports the hypothesis that near 50 wt %, the mode of EET becomes three-dimensional, thereby increasing the trapping by EFS.

Second, although the blends remain optically clear after annealing for 96 h at 413 K, there might be local phase separation for blends with higher guest concentration above 70 wt %. These guest-rich domains are probably small enough not to scatter light or be detected by conventional methods such as DSC.

Finally, the behavior of  $I_D/I_M$  as a function of guest concentration is distinctly different for miscible and immiscible blends. The curvature of  $I_D/I_M$  with increasing guest concentration may be used as a first-order fingerprint characterization for blend miscibility.

**Acknowledgment.** This work was supported by the Polymers Program of the National Science Foundation under Grant DMR 84-07847.

## References and Notes

- Frank, C. W.; Harrah, L. A. *J. Chem. Phys.* **1974**, *61*, 1526.
- Frank, C. W. *J. Chem. Phys.* **1974**, *61*, 2015.
- Frank, C. W. *Macromolecules* **1975**, *8*, 305.
- Frank, C. W.; Gashgari, M. A. *Macromolecules* **1979**, *12*, 163.
- Frank, C. W.; Gashgari, M. A.; Chutikamontham, P.; Haverly, V. J. In *Structure and Properties of Amorphous Polymers*; Walton, A. G., Ed.; Elsevier: New York, 1980; pp 187–210.
- Frank, C. W.; Gashgari, M. A. *Ann. N.Y. Acad. Sci.* **1981**, *366*, 387.
- Frank, C. W. *Plast. Compd.* Jan/Feb 1981, 67.
- Semerak, S. N.; Frank, C. W. *Macromolecules* **1981**, *14*, 443.
- Gashgari, M. A.; Frank, C. W. *Macromolecules* **1981**, *14*, 1558.
- Semerak, S. N.; Frank, C. W. *Adv. Polym. Sci.* **1983**, *54*, 32.
- Semerak, S. N.; Frank, C. W. *Adv. Chem. Ser.* **1983**, No. 203, 757.
- Gelles, R.; Frank, C. W. *Macromolecules* **1982**, *15*, 741.
- Gelles, R.; Frank, C. W. *Macromolecules* **1982**, *15*, 747.
- Semerak, S. N.; Frank, C. W. *Macromolecules* **1984**, *17*, 1148.
- Semerak, S. N.; Frank, C. W. *Can. J. Chem.* **1985**, *63*, 1328.
- Thomas, J. W.; Frank, C. W. *Macromolecules* **1985**, *18*, 1034.
- Birks, J. B. *Photophysics of Aromatic Molecules*; Wiley: London, 1970; Chapter 7.
- Flory, P. J. *Principles of Polymer Chemistry*; Cornell University Press: Ithaca, NY, 1953; Chapters 12 and 13.
- Soutar, I. *Ann. N.Y. Acad. Sci.* **1981**, *366*, 24.
- Li, X. B.; Winnik, M. A.; Guillet, J. E. *Macromolecules* **1983**, *16*, 992.
- de Gennes, P.-G. *J. Chem. Phys.* **1980**, *72*, 4756.
- Frank, C. W.; Zin, W. C. In *Photophysics of Polymers*; ACS Symposium Series 358; American Chemical Society: Washington, DC, 1987; pp 18–36.
- Gashgari, M. A.; Frank, C. W. *Macromolecules* **1988**, *21*, 2782.
- Fitzgibbon, P. D.; Frank, C. W. *Macromolecules* **1982**, *15*, 733.
- Semerak, S. N. Ph.D. Thesis, Stanford University, Stanford, CA, 1983.
- Fitzgibbon, P. D.; Frank, C. W. *Macromolecules* **1981**, *14*, 1650.
- Fredrickson, G. H.; Frank, C. W. *Macromolecules* **1983**, *16*, 572.
- Fox, T. G. *Bull. Am. Phys. Soc.* **1956**, *2*, 123.